Breast Cancer Res Treat (2008) 109:263–272
DOI 10.1007/s10549-007-9646-0

PRECLINICAL STUDY

Functional sodium iodide symporter expression in breast cancer xenografts in vivo after systemic treatment with retinoic acid and dexamethasone

Michael J. Willhauck · Bibi Sharif-Samani · Reingard Senekowitsch-Schmidtke · Nathalie Wunderlich · Burkhard Göke · John C. Morris · Christine Spitzweg

Received: 2 February 2007 / Accepted: 7 June 2007 / Published online: 18 July 2007

Abstract
Context The sodium iodide symporter (NIS) mediates iodide uptake in the thyroid gland as well as in lactating breast, and is also expressed in the majority of breast cancers. Recently, we have reported stimulation of all-*trans* retinoic acid (atRA)-induced NIS expression in the human breast cancer cell line MCF-7 by dexamethasone (Dex), resulting in an enhanced therapeutic effect of ^{131}I in vitro.
Objective In the current study we examined the efficacy of Dex stimulation of atRA-induced NIS expression in vivo in MCF-7 xenotransplants in nude mice.
Design After systemic treatment with atRA alone or in combination with Dex, iodide accumulation in the tumors was assessed by gamma camera imaging and gamma counter analysis. In addition, NIS expression was examined on RNA and protein level by RT-PCR and immunohistochemistry, respectively.
Results Using gamma camera imaging after intraperitoneal injection of 18.5 MBq ^{123}I, no iodide accumulation was detected in tumors of untreated mice or mice treated with atRA only. After combined treatment with atRA/Dex significant ^{123}I accumulation was detected in MCF-7 xenografts, which, by ex vivo gamma counting revealed a 3.3-fold increase in iodide accumulation as compared to control tumors. Surprisingly, in a subset of mice treated with atRA or atRA/Dex iodide accumulation was also detected in the normal mammary glands. In a normal human mammary epithelial cell line HB-2, however, no functional NIS expression was induced after treatment with atRA and/or Dex in vitro. Further, NIS mRNA and protein expression was detected in atRA/Dex treated MCF-7 tumors by RT-PCR and immunohistochemistry, respectively.
Conclusion Treatment with Dex in the presence of atRA is able to induce significant amounts of iodide accumulation in breast cancer xenotransplants in vivo due to stimulation of functional NIS protein expression, which opens exciting perspectives for a possible diagnostic and therapeutic role of radioiodine in the treatment of breast cancer.

Keywords Breast cancer · Dexamethasone · Radioiodine therapy · Retinoic acid · Sodium iodide symporter

M. J. Willhauck · B. Sharif-Samani · N. Wunderlich · B. Göke · C. Spitzweg
Department of Internal Medicine II, Ludwig-Maximilians-University, Munich, Germany

R. Senekowitsch-Schmidtke
Department of Nuclear Medicine, Technical-University Munich, Munich, Germany

J. C. Morris
Department of Endocrinology, Mayo Clinic, Rochester, MN, USA

C. Spitzweg (✉)
Klinikum Grosshadern, Medizinische Klinik II, Marchioninistrasse 15, 81377 Muenchen, Germany
e-mail: Christine.Spitzweg@med.uni-muenchen.de

Introduction

Iodide trapping activity in the thyroid gland due to expression of the sodium iodide symporter (NIS) plays a key role in diagnosis and therapy of follicular cell-derived thyroid carcinomas and their metastases. As an intrinsic plasma membrane glycoprotein, NIS mediates the active transport of iodide at the basolateral membrane of thyroid follicular cells [1, 2] and thereby represents one of the oldest targets for selective radionuclide therapy. Functional expression of NIS in papillary and follicular thyroid carcinomas offers the possibility of effective imaging as

well as therapeutic destruction of tumors by ^{131}I administration contributing greatly to the generally favorable prognosis of patients with differentiated thyroid cancer, where 10-year survival rates of ~90–95% are reported.

Soon after cloning of NIS in 1996 it became clear that endogenous NIS expression is not restricted to thyroid tissue, but can also be detected in a variety of nonthyroidal tissues, such as salivary and lacrimal glands, stomach, kidney, and particularly mammary gland [1]. In normal mammary tissue NIS is present exclusively during gestation and lactation, mediating the active transport and secretion of iodide into the milk to supply iodide to the infant for the biosynthesis of thyroid hormones [3]. Hormonal regulation studies in mice showed complex regulation mechanisms for NIS in mammary gland by estrogen, prolactin, and oxytocin [4]. Similar to organification of iodide in the thyroid gland, about 20% of the trapped iodide has been shown to be organified in lactating mammary gland as a result of iodide oxidation by peroxidase expressed in the alveolar cells of the breast followed by binding to tyrosyl residues of caseins and other milk proteins [5, 6].

In contrast to the restriction of NIS expression to the lactating state in normal mammary gland, NIS expression has also been detected with high frequency in human breast cancer samples as well as in several transgenic breast cancer models, where functional activity of NIS was confirmed by scintigraphic imaging. These data indicate that NIS is frequently up-regulated during malignant transformation in breast tissue [4, 7, 8] and therefore offers a powerful tool for selective breast cancer therapy based upon NIS-targeted application of radioiodine that has been used for over 60 years in the diagnosis and therapy of follicular cell-derived thyroid cancer as the most effective anticancer radiotherapy available today.

In thyroid cancer optimal efficacy of diagnostic and therapeutic application of radioiodine requires utilization of the exquisite TSH regulation of thyroidal NIS expression through withdrawal of thyroid hormone replacement therapy or application of recombinant TSH in order to maximize NIS-mediated iodide accumulation. Therapeutic efficacy of NIS-mediated radionuclide therapy in breast cancer is therefore expected to depend on similar manipulation of mammary NIS expression. Kogai et al. were the first to show that all-*trans* retinoic acid (atRA) is able to induce both NIS gene expression as well as iodide accumulation in vitro in a well-differentiated estrogen-receptor positive human breast cancer cell line (MCF-7) [9], which was also confirmed in MCF-7 cell xenotransplants and a transgenic breast cancer mouse model in vivo [10]. MCF-7 cells are a widely used in vitro system to study regulatory mechanisms in human breast adenocarcinoma. These data that have been confirmed in subsequent studies, suggest that atRA is an absolute requirement for induction of NIS expression in MCF-7 cells [11–13]. In more recent studies, we and others have demonstrated that dexamethasone (Dex) is able to significantly enhance atRA-induced NIS expression and iodide accumulation in MCF-7 cells in vitro [12–14], that allowed to significantly increase selective cytotoxicity of ^{131}I from ~17% in MCF-7 cells treated with atRA alone to 80% in MCF-7 cells treated with Dex in the presence of atRA [14].

Based on these promising in vitro studies, in the current study we examined the effect of atRA alone and in combination with Dex on NIS expression and iodide accumulation in nude mice harboring MCF-7 cell xenografts in vivo.

Materials and methods

Cell culture

MCF-7 cells (ATCC, Manassas, VA, USA) were grown in MEM medium (Invitrogen Life Technologies Inc., Karlsruhe, Germany) supplemented with 10% fetal bovine serum (PAA, Cölbe, Germany), L-Glutamine and Penicillin/Streptomycin (Invitrogen Life Technologies Inc.) at 37°C and 5% CO_2.

HB-2 cells (a generous gift from Prof. Taylor-Papadimitrou, Cancer Research-UK Breast Cancer Biology Group, Guy's Hospital, London, UK) were cultured in DMEM with 10% FCS supplemented with hydrocortisone (5 μg/ml) and insulin (10 μg/ml) [15].

For stimulation experiments MCF-7 cells and HB-2 cells were plated into 6-well plates (3×10^5 cells/well). Twenty-four hours after plating, cells were incubated with atRA (10^{-6} M) (Sigma, Taufkirchen, Germany), and Dex (10^{-8}–10^{-7} M) (Sigma) in the presence of 10% charcoal-stripped fetal bovine serum for 24 h.

Establishment of MCF-7 xenotransplants

Xenotransplants derived from MCF-7 cells were established in female CD-1 *nu/nu* mice (Charles River Labs. Sulzfeld, Germany) by s.c. injection of 5×10^6 cells suspended in 0.15 ml of MEM and 0.15 ml of Matrigel Basement Membrane Matrix (Becton Dickinson, Bedford, MA, USA). To ensure tumor growth of the estrogen-dependent breast cancer cells, β-estradiol time-release-pellets (1.7 mg/pellet, 60-day release; Innovative Research of America, Sarasota, Fl, USA) were subcutaneously implanted. Nude mice were maintained under specific pathogen-free conditions with access to mouse chow and water ad libitum. The experimental protocol was approved by the regional governmental commission for animal protection (Regierung von Oberbayern).

Animal treatments and radioiodide uptake studies in vivo

When tumors had reached ~5 mm in diameter, β-estradiol pellets were removed, and mice were switched to a low-iodine diet and received T4 supplementation in their drinking water for 2 weeks to maximize radioiodine uptake in the tumor and reduce uptake by the thyroid gland.

For systemic treatment mice were divided into three groups (each group $n = 8$): (1) no treatment; (2) implantation of atRA-time-release pellets (160 mg/kg/day); (3) implantation of atRA (160 mg/kg/day)- and Dex (0.1 mg/day)-time-release pellets. All pellets were purchased by Innovative Research of America.

After treatment for 5 days, mice were injected with 18.5 MBq (0.5 mCi) ^{123}I and iodide accumulation was assessed using a gamma camera equipped with VXHR collimator (Forte, ADAC Laboratories, Milpitas, CA, USA). Imaging studies were performed under anesthesia using an anesthetic machine loaded with isofluoran. After imaging studies, mice were euthanized, tumors/tissues were dissected, weighed and iodide accumulation was measured using a gamma counter.

Immunohistochemistry

Immunohistochemical staining of frozen tissue sections derived from MCF-7 cell xenografts was performed using the Vectastain Elite ABC kit (Vector Laboratories, Burlingame, CA, USA). After fixation of tissue sections in cold acetone, inhibition of endogenous peroxidase activity, and blocking of nonspecific binding with blocking serum for 30 min, slides were incubated with a mouse monoclonal hNIS antibody directed against amino acid residues 468–643 of human NIS [16] at a dilution of 1:1,600 for 90 min. Tissue sections were incubated with biotin-conjugated antimouse-immunoglobulin for 30 min at room temperature, followed by incubation with streptavidin-horseradish peroxidase macromolecular complex. NovaRed (Vector Laboratories) was used as the chromogen (red precipitate). Parallel control slides were examined with the primary and secondary antibodies replaced in turn by PBS and isotype matched nonimmune IgGs.

RNA preparation and PCR amplification

Total RNA was isolated from untreated and treated MCF-7 cell xenografts or HB-2 cells using the RNeasy Mini Kit (Qiagen, Hilden, Germany) according to manufacturer's recommendations. Single stranded oligo (dT)-primed cDNA was generated using Superscript III Reverse Transcriptase (Invitrogen). Following primers were used:

hNIS (nucleotides 1,184–1,202: 5′-GATCCGCTGGCC CTGCTCATCAAC-3′: sense strand; nucleotides 1,667–1,648: 5′-AATTCGCAGGCCGGCAGGAACATTC-3′: antisense strand);

RARα (nucleotides 519–538: 5′-CTGCCAGTACTGC CGACTGC-3′: sense strand; nucleotides 729–753: 5′-ACG TTGTTCTGAGCTGTTGTTCGTA-3′: antisense strand);

RARβ (nucleotides 1,047–1,069: CACTGGCTTGACC ATCGCAGACC-3′: sense strand; nucleotides 1,507–1,527: 5′-GAGAGGTGGCATTGATCCAGG-3′: antisense strand);

RARγ (nucleotides 837–856: 5′-CTGCCAGTACTGC CGGCTAC-3′: sense strand; nucleotides 1,040–1,064: 5′-T CTGCACTGGAGTTCGTGGTATACT-3′: antisense strand);

RxRα (nucleotides: 861–882: 5′-CGACCCTGTCACC AACATTTGC-3′: sense strand; nucleotides 981–1,002: 5′-GAGCAGCTCATTCCAGCCTGCC-3′: antisense strand);

RxRβ (nucleotides 816–835: 5′-TCAGGCAAACA CTACGGGGT-3′: sense strand; nucleotides 1,566–1,585: 5′-GCATACACTTTCTCCCGCAG-3′: antisense strand);

RxRγ (nucleotides 465–484: 5′-CTCAGGAAAGCACT ACGGGG-3′: sense strand; nucleotides 804–823: 5′-CAG GGTCATTTGTCGAGTTC-3′: antisense strand).

Amplification was performed with 2 µl of each cDNA template, 50 pmol of each primer in 5 µl 10 × reaction buffer, and 0.4 units of *Platinum* Taq PCR polymerase (Invitrogen) in a final volume of 50 µl. The amplification reaction was for 30 cycles and each cycle consisted of 94°C for 45 s (denaturation), 60°C for 45 s (annealing), and 72°C for 45 s (extension) followed by a final 10 min elongation at 72°C.

To control integrity of the cDNA templates and to rule out DNA contamination carried over in the samples, all templates were amplified with intron-spanning primers that were designed to amplify a portion of the human GAPDH gene (nucleotides 368–387: 5′-GAGAA GGCTGGGGCTCATTT-3′: sense strand; nucleotides 712–695: 5′-CAGTGGGGACACGGAAGG-3′: antisense strand). The expected GAPDH product from a cDNA template is 344 bp. Reaction conditions were as stated above. PCR products were analyzed in 1.5% agarose gels (Biozym Diagnostic, Hess. Oldendorf, Germany) stained with ethidium bromide (Sigma-Aldrich). The number of amplification cycles was determined such that the product amplification was in the exponential phase. For each RT-Mix, GAPDH was co-amplified with the target gene to confirm equal amounts of starting cDNA.

Following PCR amplification, PCR products were gel-purified using the Agarose Gel DNA Extraction Kit (Boehringer Mannheim) and subjected to automated sequencing.

Iodide uptake studies in vitro in HB-2 cells

Uptake of ^{125}I by treated MCF-7 cells and untreated as well as treated HB-2 cells was determined at steady-state conditions as described by Weiss et al. [17]. In brief, cells were plated on 6-well plates (3×10^5 cells/well), and following incubation with atRA (10^{-6} M) and Dex (10^{-8}–10^{-7} M), respectively, iodide uptake studies were performed in Hanks' balanced salt solution (HBSS) supplemented with 10 μM NaI, 3.7 MBq (0.1 μCi) Na ^{125} I/ml, and 10 mM HEPES (pH 7.3). A 100 μM concentration of $KClO_4$ was added to control wells. Following incubation for 1 h, trapped iodide was removed from cells by a 20-min incubation in 1 N NaOH and measured by γ-counting. Results were normalized to cell survival measured by cell viability assay (see below) and expressed as cpm/A490 nm.

Cell viability assay

Cell viability was measured using the commercially available MTS-assay (Promega Corp., Mannheim, Germany) according to the manufacturer's recommendations. Cells were incubated with freshly prepared MTS [3-(4,5-dimethylthiazol)-2-yl-5-(3-carboxymeth-oxyphenyl)-2-(4-sulfophenyl)-2H-tetrazolium)]/phenazine methosulfate solution (ratio 1:1 by volume) for 1.5 h at 37°C in a humidified 5% CO_2 atmosphere. The absorbance of the formazan product was read at 490 nm, which is directly proportional to the number of living cells in culture.

Membrane preparation and Western blot analysis

Cell membranes were prepared from treated and untreated HB-2 cells by a modification of a previously described procedure [14, 18]. For Western blot analysis, the NuPAGE electrophoresis system (Invitrogen) was used. Equal amounts of membrane protein as determined by DC protein assay (20 μg) (Bio-Rad, Hercules, CA, USA) were reduced by incubation with 0.5 M dithiothreitol for 10 min at 70°C and loaded on 4–12% Bis–Tris–HCl buffered polyacrylamide gels. Following gel electrophoresis for 1 h, proteins were transferred to nitrocellulose membranes using electroblotting. Following blotting, membranes were preincubated for 1 h in 5% low-fat dried milk in TBS-T (20 mM Tris, 137 mM NaCl, and 0.1% Tween-20) to block nonspecific binding sites. Membranes were then incubated with a mouse monoclonal antibody directed against amino acid residues 468–643 of human NIS (dilution 1:3,000) [16] for 2 h at room temperature. After washing with TBS-T, horseradish peroxidase-labeled goat-antimouse antibody was applied (dilution 1:5,000) for 1 h at room temperature before incubation with enhanced chemiluminescence Western blotting detection reagents (Amersham, Piscataway, NJ, USA) for 1 min. Exposures were made at room temperature for ~1 min using BIOMAX MR films (Sigma). Prestained protein molecular weight standards (Bio-Rad) were run in the same gels for comparison of molecular weight and estimation of transfer efficiency.

Results

Radioiodine uptake studies in vivo in MCF-7 xenografts

Two weeks after application of a low-iodine diet and T4 supplementation and removal of the β-estradiol pellets (tumor size ≥ 5 mm in diameter) three groups of mice were established: (1) no treatment; (2) atRA treatment; (3) atRA/Dex treatment. After a 5-day treatment period, mice received 18.5 MBq (0.5 mCi) ^{123}I by i.p. injection and were imaged using a gamma camera. No iodide accumulation was detected in tumors of untreated mice (Fig. 1a) or mice treated with atRA (Fig. 1b) or Dex alone (data not shown). In contrast, significant iodide accumulation was observed in MCF-7 xenografts of mice following s.c. implantation of atRA/Dex pellets (in six of eight mice) with accumulation of ~2–5% of the total radioiodine dose administered (Fig. 1c, arrows). Surprisingly, in 25% of the atRA-treated and in 75% of the atRA/Dex-treated mice iodide uptake was also observed in the normal mammary glands (Fig. 1b, c, arrows). The radioiodide uptake induced by atRA or atRA/Dex was inhibited by injection of $NaClO_4$ (2 mg/mouse), a specific competitive inhibitor of NIS-mediated iodide transport. The average biological half-life of accumulated radioiodine in MCF-7 xenografts as determined by serial imaging was ~2–3 h. In comparison, ~12 and 15% of the total radioiodine dose were accumulated in the thyroid gland and stomach, respectively. The iodide uptake in stomach was significantly higher than usually seen in humans, which may be a result of increased NIS expression in the murine gastric mucosa and may also result from pooling of gastric juices as the mice were anesthetized for a prolonged period for serial imaging. In addition, in our earlier studies in prostate cancer xenografts after PSA promoter-targeted NIS gene transfer, similar iodide accumulation was reported in the thyroid gland and stomach without any adverse effects after application of a therapeutic dose of 111 MBq ^{131}I [19].

Control mice without prior injection of tumor cells and/or implantation of estradiol pellets also revealed iodide accumulation in normal mammary glands in a subset of mice following systemic treatment with atRA or atRA/Dex, while mice without treatment showed no iodide accumulation in normal mammary glands (data not shown).

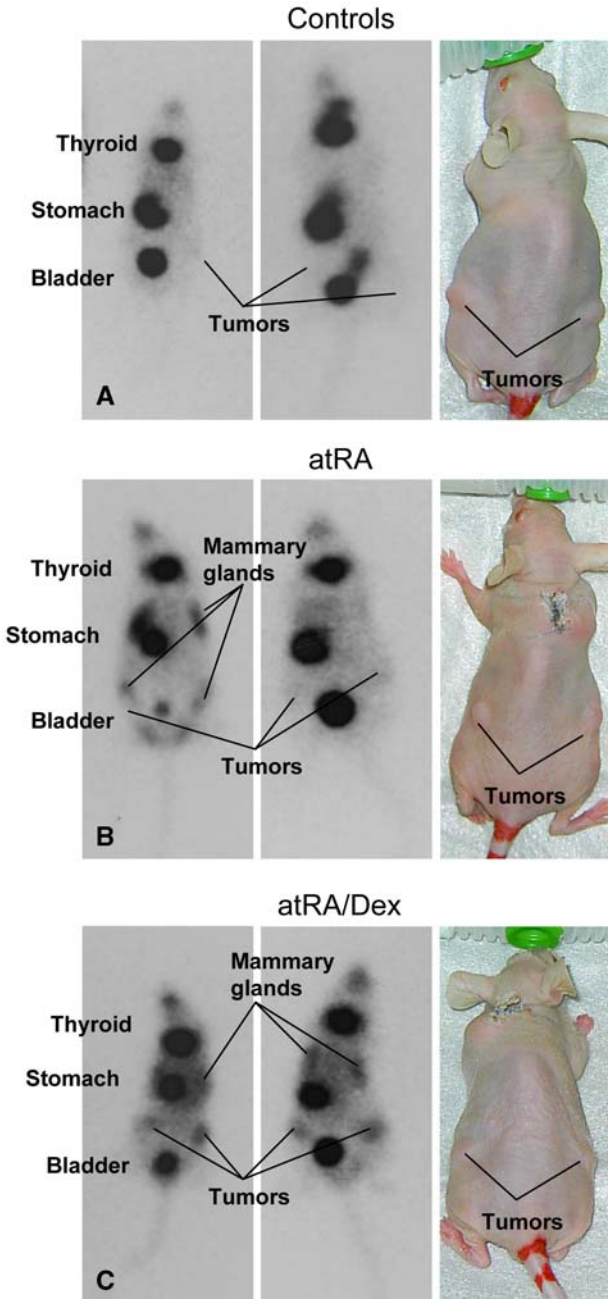

Fig. 1 Radioiodide uptake studies in vivo. ^{123}I scan of a mouse harboring MCF-7 cell xenografts 2 h following i.p. injection of 18.5 MBq (500 μCi) ^{123}I. While no iodide accumulation was detected in tumors of untreated mice (**a**) and mice treated with atRA alone (**b**), significant iodide accumulation was observed in MCF-7 xenografts of mice following s.c. implantation of atRA/Dex pellets (**c**). Surprisingly, iodide uptake was also detected in normal mammary glands in a subset of mice (**b**, **c**). ^{123}I was also accumulated physiologically in bladder, stomach, thyroid and salivary glands

No significant retinoid toxicity (skin scaling, weight loss) was observed in mice treated with atRA alone for 5 days. Combined treatment with atRA/Dex, however, was associated with mild side effects, such as weight loss and skin scaling, which were not life limiting and reversible upon rehydration.

Radioiodine uptake studies ex vivo in MCF-7 xenografts

After imaging mice were sacrificed, tumors dissected and ^{123}I accumulation was measured by gamma counting. Iodide accumulation was significantly increased up to 3.3-fold ($P < 0.05$) in MCF-7 xenotransplants following systemic atRA/Dex treatment (Fig. 2) as compared to control tumors, tumors treated with atRA/Dex plus perchlorate and tumors treated with atRA alone, that revealed mild iodide accumulation only in one of eight mice.

Analysis of NIS protein expression in MCF-7 xenografts by immunohistochemistry

Immunohistochemical staining of frozen tissue sections derived from untreated (Fig. 3a), atRA- (Fig. 3b) and atRA/Dex- treated (Fig. 3c) MCF-7 xenotransplant tumors using a mouse monoclonal hNIS-specific antibody showed strong but heterogenous and primarily membrane-associated hNIS-specific immunoreactivity in xenografts following treatment with atRA in combination with Dex (Fig. 3c, arrows). No treatment or treatment with atRA alone did not result in hNIS-specific immunoreactivity (Fig. 3a, b). Parallel control slides with the primary and secondary antibodies replaced in turn by PBS and isotype-matched nonimmune immunoglobulin were negative (not shown).

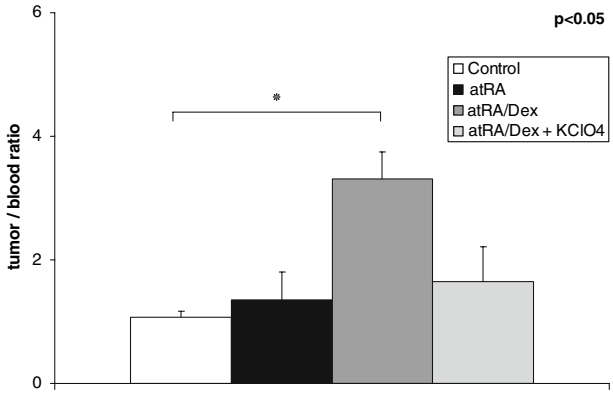

Fig. 2 Radioiodide uptake studies ex vivo. After imaging mice were sacrificed, tumors dissected and ^{123}I accumulation was measured by gamma counting. Data were normalized to the weight of each tumor and presented as tumor/blood ratio. Iodide accumulation was significantly increased up to 3.3-fold ($P < 0.05$) in MCF-7 xenotransplants following systemic atRA/Dex treatment as compared to control tumors and tumors treated with atRA alone, that revealed mild iodide accumulation only in one of eight mice

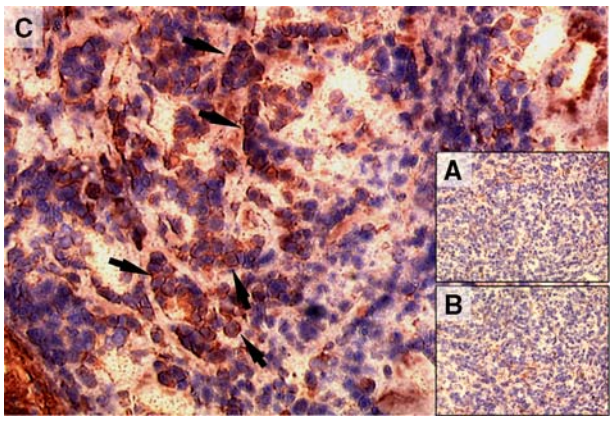

Fig. 3 Immunohistochemistry. Immunohistochemical staining of frozen tissue sections derived from untreated (**a**), atRA- (**b**) and atRA/Dex- treated (**c**) MCF-7 xenotransplant tumors using a mouse monoclonal hNIS-specific antibody showed strong but heterogenous and primarily membrane-associated hNIS-specific immunoreactivity in xenografts following treatment with atRA in combination with Dex (Fig. 3c, *arrows*). No treatment or treatment with atRA alone did not result in hNIS-specific immunoreactivity (Fig. 3a, b). Parallel control slides with the primary and secondary antibodies replaced in turn by PBS and isotype-matched nonimmune immunoglobulin were negative (not shown) (magnification × 200)

Analysis of NIS and retinoid receptor RNA expression in MCF-7 xenografts by PCR amplification

To investigate the effect of atRA and Dex on NIS RNA expression in MCF-7 cell xenografts in vivo, tumor specimens were processed for RNA preparation followed by RT-PCR with a pair of hNIS-specific oligonucleotide primers to amplify a 483 bp fragment of the hNIS DNA (Fig. 4, top). To monitor cDNA integrity and quantity, samples were co-amplified with a pair of human GAPDH primers (Fig. 4, bottom). RT-PCR revealed hNIS gene expression at low level in MCF-7 tumors derived from untreated and atRA treated mice, which was significantly increased ~5-fold in MCF-7 cell xenografts derived from atRA/Dex treated mice. Sequencing of the PCR products revealed full identity with the published human thyroid-derived NIS cDNA sequence [20].

In addition, using RT-PCR, gene expression of retinoic acid receptors RARα, RARβ, and RARγ as well as retinoid x receptors RxRα, RxRβ, and RxRγ was demonstrated in MCF-7 xenografts (Fig. 5).

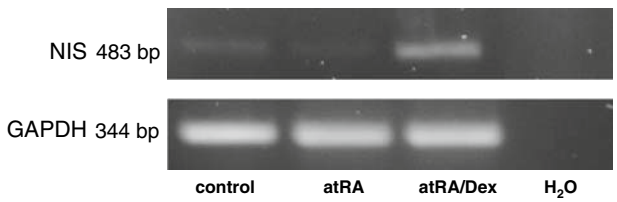

Fig. 4 Analysis of NIS RNA expression in MCF-7 xenografts by PCR amplification. RT-PCR using a pair of hNIS-specific oligonucleotide primers to amplify a 483 bp fragment of the hNIS DNA (*top*) revealed hNIS RNA expression at low level in MCF-7 tumors derived from untreated and atRA treated mice, which was significantly increased ~5-fold in MCF-7 cell xenografts derived from atRA/Dex treated mice. To monitor cDNA integrity and quantity, samples were co-amplified with a pair of GAPDH primers (*bottom*)

Iodide uptake studies in vitro in HB-2 cells

The effect of Dex (10^{-8}–10^{-7} M) in the presence of atRA (10^{-6} M) on iodide accumulation in MCF-7 and HB-2 cells was examined by iodide uptake assay. In contrast to a significant stimulation of iodide accumulation in MCF-7 cells after treatment with atRA/Dex, no perchlorate-sensitive iodide uptake above background level was observed in untreated HB-2 cells and in HB-2 cells treated with Dex or atRA alone, which was not changed after combined treatment with atRA/Dex (Fig. 6).

Analysis of NIS RNA expression in HB-2 cells by PCR amplification

After incubation of HB-2 cells for 24 h with Dex (10^{-7} M) in the absence or presence of atRA (10^{-6} M), NIS mRNA levels were examined by RT-PCR using a pair of hNIS-specific oligonucleotide primers to amplify a 483 bp fragment of the hNIS DNA, that revealed no hNIS gene expression in untreated HB-2 cells or in HB-2 cells treated with atRA alone or atRA/Dex. In contrast, MCF-7 cells stimulated with atRA/Dex revealed NIS gene expression as detected by a single band of 483 bp. To monitor cDNA integrity and quantity, samples were co-amplified with a pair of GAPDH primers (data not shown).

Analysis of NIS protein expression in HB-2 cells by Western blot analysis

After incubation of HB-2 cells for 24 h with Dex (10^{-7} M) in the presence or absence of atRA (10^{-6} M), NIS protein

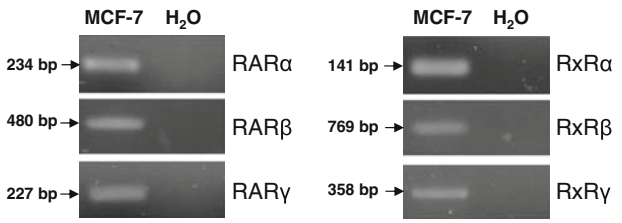

Fig. 5 Analysis of retinoid receptor RNA expression in MCF-7 xenografts by PCR amplification. RT-PCR of mRNA obtained from untreated MCF-7 xenotransplants 8–12 weeks following transplantation revealed expression of retinoic acid receptors RARα, RARβ, and RARγ as well retinoid x receptors RxRα, RxRβ, and RxRγ

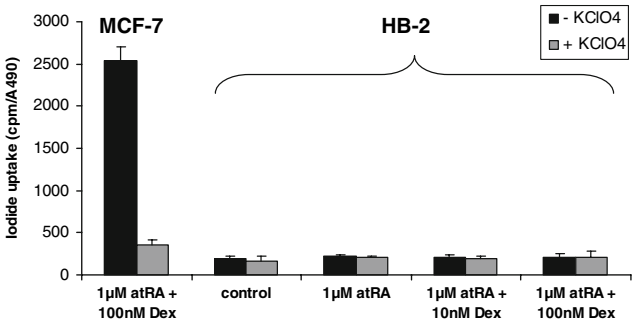

Fig. 6 Iodide uptake studies in vitro in HB-2 cells. Effect of Dex (10^{-8}–10^{-7} M) in the presence of atRA (10^{-6} M) on iodide accumulation in MCF-7 and HB-2 cells. In contrast to significant stimulation of iodide accumulation in MCF-7 cells after treatment with atRA/Dex, no perchlorate-sensitive iodide uptake above background level was observed in untreated HB-2 cells (control) and in HB-2 cells treated with atRA alone or after combined atRA/Dex treatment. Results have been normalized to living cells measured by MTS cell viability assay, which directly correlates with number of living cells. Results represent mean ± SD of triplicate experiments, and are expressed as amount of iodide accumulation in counts per minute cpm/A490 nm

expression levels were examined in HB-2 cells by Western blot analysis using a mouse monoclonal human NIS-specific antibody. NIS protein was detected as a band of ~90 kDa in the positive control (MCF-7 cells treated with atRA/Dex), while no NIS protein expression was detected in untreated HB-2 cells and cells treated with atRA alone or in combination with Dex (data not shown).

Discussion

Based on our encouraging in vitro data on stimulation of atRA-induced NIS expression and iodide accumulation in the estrogen-receptor positive human breast cancer cell line MCF-7 [14], the aim of the present study was to examine the effect of treatment with atRA and Dex on NIS expression and iodide accumulation in vivo in MCF-7 xenotransplants in CD1 nude mice. In our in vivo model only the systemic combined treatment with atRA and Dex was able to induce a significant amount of iodide accumulation based on stimulation of NIS mRNA and protein expression.

Cloning of the NIS gene in 1996 and its extensive characterization has provided us with a powerful new diagnostic and therapeutic gene, that allowed the development of a promising cytoreductive gene therapy strategy based on NIS gene transfer in extrathyroidal tumors [1, 19–29]. In breast cancer Dwyer et al. used the tumor-specific MUC1-promoter to target NIS expression to breast cancer cells and demonstrated a 83% tumor volume reduction after adenoviral NIS gene transfer into breast cancer xenografts followed by ^{131}I application [30].

In contrast to exogenously induced extrathyroidal iodide accumulation by NIS gene transfer, endogenous iodide accumulation in breast tissue was first reported 50 years ago [31] and was later discovered to be mediated by NIS expressed in lactating mammary gland [4, 32–36]. While normal mammary gland epithelial cells express NIS physiologically only during late gestation and lactation, Tazebay et al. were the first to demonstrate functional NIS expression in experimental mammary adenocarcinomas in transgenic mouse models. Furthermore, NIS protein expression was detected in 20 of 23 (87%) invasive carcinomas and five of six (83%) ductal in situ carcinomas [4]. Long before the cloning of NIS and detection of NIS expression in human breast it was known that breast atypia and malignancy reveal increased radioiodine uptake and that breast cancers can be detected by radioiodine/^{99m}Tc scintigraphy [37–39]. In support of these data, using immunohistochemistry Rudnicka et al., were able to detect NIS protein expression in 45 of 50 specimens of invasive ductal breast carcinomas (90%) [7].

The high prevalence of NIS in human breast cancer and the demonstration of functionally active NIS expression in breast cancer tissue in transgenic breast cancer mouse models suggest that endogenous mammary NIS expression may offer the possibility of NIS-targeted radioiodide imaging and therapy in breast cancer similar to its application in thyroid cancer. Based on these data, a clinical trial was performed by Nancy Carrasco's group, in which 27 women with breast cancer metastases were scanned with ^{99m}Tc-pertechnetate or ^{123}I to assess functional NIS activity in their metastases after thyroidal NIS expression was down-regulated by application of T3 alone or in combination with methimazole. However, only eight tumors revealed NIS expression which resulted in radionuclide accumulation in only two of the eight tumors [40]. Similarly, Moon et al. examined ^{99m}Tc-pertechnetate accumulation and NIS mRNA expression in 25 breast tumors and found significantly increased ^{99m}Tc-pertechnetate uptake in only four tumors, while all of the 25 tumors revealed NIS mRNA expression [8]. These data strongly suggest that stimulation of mammary NIS expression will be necessary to maximize diagnostic and therapeutic efficacy of NIS-mediated radioiodide accumulation in breast cancer, similar to TSH stimulation of thyroidal NIS, that is required for maximizing sensitivity and efficiency of radioiodide application in diagnosis and therapy of thyroid cancer.

Kogai et al. were the first to report stimulation of functional NIS expression in the human breast cancer cell line MCF-7 in vitro after administration of various retinoid receptor ligands [9]. In a more recent study, the same group was able to confirm induction of NIS mRNA and protein expression after systemic treatment with atRA resulting in

increased iodide accumulation in MCF-7 xenotransplant tumors in SCID mice as well as in a transgenic breast cancer mouse model (MMTV-PyVT) [10].

While the exact mechanisms that are responsible for atRA-induced NIS expression are not known, Dentice et al. identified the transcription factor Nkx-2.5, a potent inducer of the NIS promoter, as a novel important transcriptional regulator of mammary NIS that is involved in retinoic acid-induced NIS expression in mammary gland [41].

In a recent study, we examined the effect of Dex on the atRA-induced NIS expression and iodide accumulation in MCF-7 cells in vitro and demonstrated a significant stimulation of NIS mRNA and protein expression after incubation with Dex in the presence of atRA resulting in a three- to fourfold increase of iodide accumulation accompanied with a mild reduction of iodide efflux. Ultimately these effects allowed a significantly stimulated therapeutic effect of ^{131}I in a clonogenic assay [14]. Similar data were reported by Kogai et al. [12] and Dohan et al. [13], suggesting that combined treatment with atRA and Dex may allow diagnostic and therapeutic application of radioiodine in breast cancer in the future.

In view of these in vitro data, in the current study we examined the efficacy of Dex stimulation of atRA-induced NIS expression in vivo in MCF-7 xenotransplants in CD1 nude mice. While in our study, using a single dose and time regimen for atRA and Dex, no functional NIS protein expression could be detected in tumors of untreated mice or mice treated with atRA or Dex alone, NIS mRNA and protein expression was significantly enhanced in tumors after 5 days of systemic treatment with atRA in combination with Dex. Moreover, NIS expression in atRA/Dex treated tumors resulted in significant ^{123}I accumulation demonstrated by gamma camera imaging as well as ex vivo gamma counting of dissected tumors, that revealed a 3.3-fold increase of iodide accumulation as compared to control tumors and tumors treated with atRA only. Although it has to be taken into consideration, that only one dose and time regimen was used for atRA/Dex treatment in our experiments, we were able to confirm our data from the in vitro studies, that showed only mild induction of functional NIS expression in MCF-7 cells after atRA-treatment alone and pronounced stimulation of NIS expression and iodide accumulation after combined atRA/Dex treatment [14].

In contrast to our data, Kogai et al. demonstrated the induction of NIS-mediated iodide accumulation in vivo in MCF-7 cell xenografts in SCID mice after treatment with atRA only [10]. These differences between our and Kogai's data might be due to different strains of MCF-7 cells that were used in our studies, and should be investigated in further studies also addressing dose- and time-dependency of atRA and Dex effects. Furthermore, Kogai et al. did not observe any iodide accumulation in normal mammary glands in their MCF-7 xenotransplant model in SCID mice [10], while in our MCF-7 xenograft model in CD1 nude mice we have detected iodide accumulation in normal mammary glands in ~20% of the atRA-treated mice and almost 75% of the atRA/Dex-treated mice. In our experiments the estradiol-pellets that were implanted to enhance growth of MCF-7 cells in vivo were removed 2 weeks before atRA/Dex treatment and imaging studies, to rule out estradiol-induced NIS expression in normal mammary gland. Moreover, CD1 nude mice without any tumors and without implantation of estradiol pellets were imaged after treatment with atRA only or combined treatment with atRA/Dex and also revealed iodide accumulation in their normal mammary glands. This observation, that is discrepant to the data of Kogai et al. and would hamper the diagnostic and therapeutic potential of atRA/Dex-induced NIS expression in breast cancer, might be mouse-specific resulting from different regulation mechanisms of NIS expression in normal mammary gland in the different mouse models used in these studies. To address this issue in the human situation, our preliminary experiments in a human nontumorigenic mammary epithelial cell line HB-2 showed no induction of NIS expression or iodide accumulation in vitro after incubation with atRA and/or Dex. Possible differences in the transcriptional regulation of NIS in these two cell lines (MCF-7 and HB-2) might be responsible for this observation, and need to be addressed in future studies.

A general concern in the course of therapeutic radionuclide application is whether a selective tumor absorbed dose can be achieved that is high enough to allow a therapeutic effect. In our study ~2–5% of the total radioiodide administered was accumulated by the breast cancer xenografts after treatment with atRA/Dex with a biological half life of about 2–3 h. In one of our earlier studies on adenovirus mediated NIS gene transfer in prostate carcinoma xenografts in vivo we were able to show that a tumor radioiodine uptake of 20% with a biological half-life of 5.6 h is sufficient for an average tumor volume reduction of 85% after application of a therapeutic ^{131}I dose even in the absence of iodide organification [25]. These data clearly showed, that iodide organification, which does occur in the mammary gland based on iodide oxidation by lactoperoxidases and iodide binding to casein [5], but has not been demonstrated in MCF-7 cells [9], is not an absolute prerequisite for effective radioiodine therapy. Whether the level of atRA/Dex-induced endogenous NIS expression and iodide accumulation in MCF-7 xenotransplants is high enough to allow a therapeutic effect needs to be addressed in further studies. The well known additional antiproliferative and radiosensitizing effects of retinoids in breast cancer cells [42–45] as well as the bystander effect caused

by the crossfire effect of β-particles emitted by ^{131}I are able to potentiate the therapeutic effect of ^{131}I in vivo [46, 47]. Should limited iodide accumulating capacity and short iodide retention limit therapeutic efficacy of ^{131}I in breast cancer, the application of alternative radionuclides, including the high energy α-emitter ^{211}Astatine (^{211}At) and the potent β-emitter ^{188}Rhenium (^{188}Re), that are also transported by NIS, can be considered for application following atRA/Dex-mediated induction of endogenous NIS expression in breast cancer due to their higher energy and shorter half-life, thereby offering the possibility of higher energy deposition in a shorter time period [48–53]. Stimulation of the tumor absorbed radiation dose and the therapeutic effect of NIS-mediated radionuclide therapy has already been demonstrated for ^{188}Re in NIS-expressing mammary adenocarcinomas in a transgenic mouse model [48, 49, 51, 52].

In conclusion, in the current study we were able to confirm our previous in vitro data and demonstrated that Dex is capable of increasing atRA-induced endogenous NIS expression levels, thereby significantly enhancing iodide accumulation in MCF-7 breast cancer xenotransplants. Therefore, based on the extensive experience with radioiodine application in diagnosis and therapy of thyroid cancer as the most effective targeted radiotherapy available today, induction of NIS expression after combined treatment with Dex and atRA may represent a powerful strategy for breast-selective pharmacological modulation of functional NIS expression in breast cancer in order to improve the feasibility of using endogenous NIS expression in breast cancer as novel target for selective radioiodine imaging as well as therapy.

Acknowledgments This study was supported by grants to C. Spitzweg (Sp 581/3–2, Sp 581/4-1, Sp 581/4-2 (Forschergruppe FOR-411) from the German Research Council (Deutsche Forschungsgemeinschaft, Bonn, Germany), and by the FöFoLe-Program of the Ludwig-Maximilians-University Munich to M.J. Willhauck (FöFoLe Reg.Nr. 442).

References

1. Spitzweg C, Morris JC (2002) The sodium iodide symporter: its pathophysiological and therapeutic implications. Clin Endocrinol 57:559–574
2. Dohan O, De la Vieja A, Paroder V, Riedel C, Artani M, Reed M, Ginter CS, Carrasco N (2003) The sodium/iodide symporter (NIS): characterization, regulation, and medical significance. Endocrine Rev 24:48–77
3. Carrasco N (1993) Iodide transport in the thyroid gland. Biochem Biophys Acta 1154:65–82
4. Tazebay UH, Wapnir IL, Levy O, Dohan O, Zuckier LS, Zhao QH, Deng HF, Amenta PS, Fineberg S, Pestell RG, Carrasco N (2000) The mammary gland iodide transporter is expressed during lactation and in breast cancer. Nature Med 6:871–878
5. Strum JM (1978) Site of iodination in rat mammary gland. Anat Rec 192:235–244
6. Strum JM, Phelps PC, McAtee MM (1983) Resting human female breast tissue produces iodinated proteins. J Ultrastruct Res 84:130–139
7. Rudnicka L, Sinczak A, Szybinski P, Huszno B, Stachura J (2003) Expression of the Na(+)/I(-) symporter in invasive ductal breast cancer. Folia Histochem Cytobiol 41:37–40
8. Moon DH, Lee SJ, Park KY, Park KK, Ahn SH, Pai MS, Chang H, Lee HK, Ahn I-M (2001) Correlation between 99mTc-pertechnetate uptakes and expressions of human sodium iodide symporter gene in breast tumor tissues. Nucl Med Biol 28: 829–834
9. Kogai T, Schultz J, Johnson L, Huang M, Brent G (2000) Retinoic acid induces sodium/iodide symporter gene expression and radioiodide uptake in the MCF-7 breast cancer cell line. Proc Natl Acad Sci USA 97:8519–8524
10. Kogai T, Kanamoto Y, Che LH, Taki K, Moatamed F, Schultz JJ, Brent GA (2004) Systemic retinoic acid treatment induces sodium/iodide symporter expression and radioiodine uptake in mouse breast cancer models. Cancer Res 64:415–422
11. Tanosaki S, Ikezoe T, Heaney A, Said JW, Dan K, Akashi M, Koeffler P (2003) Effect of ligands of nuclear hormone receptors on sodium/iodide symporter expression and activity in breast cacner cells. Breast Cancer Res Treat 79:335–345
12. Kogai T, Kanamoto Y, Li AI, Che LH, Ohashi E, Taki K, Chandraratna RA, Saito T, Brent GA (2005) Differential regulation of sodium/iodide symporter gene expression by nuclear receptor ligands in MCF-7 breast cancer cells. Endocrinology 146:3059–3069
13. Dohan O, De la Vieja A, Carrasco N (2006) Hydrocortisone and purinergic signaling stimulate NIS-mediated iodide transport in breast cancer cells. Mol Endocrinol 20:1121–1137
14. Unterholzner S, Willhauck MJ, Cengic N, Schütz M, Göke B, Morris JC, Spitzweg C (2006) Dexamethasone stimulation of retinoic acid-induced sodium iodide symporter expression and cytotoxicity of 131-I in breast cancer cells. J Clin Endocrinol Metab 91:69–78
15. Berdichevsky F, Alford D, D'Souza B, Taylor-Papadimitriou J (1994) Branching morphogenesis of human mammary epithelial cells in collagen gels. J Cell Sci 107:3557–3568
16. Castro MR, Bergert ER, Beito TG, Roche PC, Ziesmer SC, Jhiang SM, Goellner JR, Morris JC (1999) Monoclonal antibodies against the human sodium iodide symporter: utility for immunocytochemistry of thyroid cancer. J Endocrinol 163:495–504
17. Weiss SJ, Philip NJ, Grollmann EF (1984) Iodine transport in a continous line of cultured cells from rat thyroid. Endocrinology 114:1090–1098
18. Kaminsky SM, Levy O, Salvador C, Dai G, Carrasco N (1994) Na^+-I^- symport activity is present in membrane vesicles from thyrotropin-deprived non-I-transporting cultured thyroid cells. Proc Natl Acad Sci USA 91:3789–3793
19. Spitzweg C, O'Connor MK, Bergert ER, Tindall DJ, Young CYF, Morris JC (2000) Treatment of prostate cancer by radioiodine therapy after tissue-specific expression of the sodium iodide symporter. Cancer Res 60:6526–6530
20. Smanik PA, Liu Q, Furminger TL, Ryu K, Xing S, Mazzaferri EL, Jhiang SM (1996) Cloning of the human sodium iodide symporter. Biochem Biophys Res Commun 226:339–345
21. Dai G, Levy O, Carrasco N (1996) Cloning and characterization of the thyroid iodide transporter. Nature 379:458–460
22. Smanik PA, Ryu K-Y, Theil KS, Mazzaferri EL, Jhiang SM (1997) Expression, exon-intron organization, and chromosome mapping of the human sodium iodide symporter. Endocrinology 138:3555–3558
23. Spitzweg C, Harrington KJ, Pinke LA, Vile RG, Morris JC (2001) The sodium iodide symporter and its potential in cancer therapy. J Clin Endocrinol Metab 86:3327–3335

24. Spitzweg C, Zhang S, Bergert ER, Castro MR, McIver BD, Tindall DJ, Young CYF, Morris JC (1999) Prostate-specific antigen (PSA) promoter-driven androgen-inducible expression of sodium iodide symporter in prostate cancer cell lines. Cancer Res 59:2136–2141
25. Spitzweg C, Dietz AB, O'Connor MK, Bergert ER, Tindall DJ, Young CYF, Morris JC (2001) In vivo sodium iodide symporter gene therapy of prostate cancer. Gene Ther 8:1524–1531
26. Kakinuma H, Bergert ER, Spitzweg C, Cheville JC, Lieber MM, Morris JC (2003) Probasin promoter (ARR2PB)-driven, prostate-specific expression of h-NIS for targeted radioiodine therapy of prostate cancer. Cancer Res 63:7840–7844
27. Spitzweg C, Scholz IV, Bergert ER, Tindall DJ, Young CYF, Göke B, Morris JC (2003) Retinoic acid-induced stimulation of sodium iodide symporter (NIS) expression and cytotoxicity of radioiodine in prostate cancer cells. Endocrinology 144: 3423–3432
28. Cengic N, Baker CH, Schutz M, Göke B, Morris JC, Spitzweg C (2005) A novel therapeutic strategy for medullary thyroid cancer based on radioiodine therapy following tissue-specific sodium iodide symporter gene expression. J Clin Endocrinol Metab 90:4457–4464
29. Scholz IV, Cengic N, Baker CH, Harrington KJ, Maletz K, Bergert ER, Vile R, Göke B, Morris JC, Spitzweg C (2005) Radioiodine therapy of colon cancer following tissue-specific sodium iodide symporter gene transfer. Gene Ther 12:272–280
30. Dwyer RM, Bergert ER, O'Connor MK, Gendler SJ, Morris JC (2005) In vivo radioiodide imaging and treatment of breast cancer xenografts after MUC1-driven expression of the sodium iodide symporter. Clin Cancer Res 11:1483–1489
31. Brown-Grant K (1957) The iodide concentrating mechanism of the mammary gland. J Physiol 135:644–654
32. Spitzweg C, Joba W, Schriever K, Goellner JR, Morris JC, Heufelder AE (1999) Analysis of human sodium iodide symporter immunoreactivity in human exocrine glands. J Clin Endocrinol Metab 84:4178–4184
33. Spitzweg C, Joba W, Eisenmenger W, Heufelder AE (1998) Analysis of human sodium iodide symporter gene expression in extrathyroidal tissues and cloning of its complementary deoxyribonucleic acids from salivary gland, mammary gland, and gastric mucosa. J Clin Endocrinol Metab 83:1746–1751
34. Spitzweg C, Dutton CM, Castro MR, Bergert ER, Goellner JR, Heufelder AE, Morris JC (2001) Expression of the sodium iodide symporter in human kidney. Kidney Int 59:1013–1023
35. Wapnir IL, Rijn M, Nowels K, Amenta PS, Walton K, Montgomery K, Greco RS, Dohan O, Carrasco N (2003) Immunohistochemical profile of the sodium/iodide symporter in thyroid, breast, and other carcinomas using high density tissue microarrays and conventional sections. J Clin Endocrinol Metab 88:1880–1888
36. Jhiang SM, Cho J-Y, Ryu K-Y, De Young BR, Smanik PA, McGaughy VR, Fischer AH, Mazzaferri EL (1998) An immunohistochemical study of Na+/I- symporter in human thyroid tissues and salivary gland tissues. Endocrinology 139:4416–4419
37. Eskin BA, Parker JA, Bassett JG, George DL (1974) Human breast uptake of radioactive iodine. Obstet Gynecol 44:398–402
38. Eskin BA (1977) Iodine and mammary cancer. Adv Exp Med Biol 91:293–304
39. Cancroft ET, Goldsmith SJ (1973) 99mTc-pertechnetate scintigraphy as an aid in the diagnosis of breast masses. Radiology 106:441–444
40. Wapnir IL, Goris M, Yudd A, Dohan O, Adelman D, Nowels K, Carrasco N (2004) The Na+/I- symporter mediates iodide uptake in breast cancer metastases and can be selectively down-regulated in the thyroid. Clin Cancer Res 10:4294–4302
41. Dentice M, Luongo C, Elefante A, Romino R, Ambrosio R, Vitale M, Rossi G, Fenzi G, Salvatore D (2004) Transcription factor Nkx-2.5 induces sodium/iodide symporter gene expression and participates in retinoic acid- and lactation-induced transcription in mammary cells. Mol Cell Biol 24:7863–7877
42. Czeczuga-Semeniuk E, Wolczynski S, Dzieciol J, Dabrowska M, Anchim T, Tomaszewska I (2001) 13-cis retinoic acid and all-trans retinoic acid in the regulation of the proliferation and survival of human breast cancer cell line MCF-7. Cell Mol Biol Lett 6:925–939
43. Van Heusden J, Wouters W, Ramaekers FC, Krekels MD, Dillen L, Borgers M, Smets G (1998) All-trans-retinoic acid metabolites significantly inhibit the proliferation of MCF-7 human breast cancer cells in vitro. Br J Cancer 77:26–32
44. Mangiarotti R, Danova M, Alberici R, Pellicciari C (1998) All-trans retinoic acid (ATRA)-induced apoptosis is preceded by G1 arrest in human MCF-7 breast cancer cells. Br J Cancer 77:186–191
45. Rutz HP, Little JB (1989) Modification of radiosensitivity and recovery from X ray damage in vitro by retinoic acid. Int J Radiat Oncol Biol Phys 16:1285–1288
46. Carlin S, Cunningham SH, Boyd M, McCluskey AG, Mairs RJ (2000) Experimental targeted radioiodide therapy following transfection of the sodium iodide symporter gene: effect on clonogenicity in both two- and three-dimensional models. Cancer Gene Ther 7:1529–1536
47. Mitrofanova E, Hagan C, Qi J, Seregina T, Link C (2003) Sodium iodide symporter/radioactive iodine system has more efficient antitumor effect in three-dimensional spheroids. Anticancer Res 23:2397–2404
48. Dadachova E, Bouzahzah B, Zuckier LS, Pestell RG (2002) Rhenium-188 as an alternative to iodine-131 for treatment of breast tumors expressing the sodium/iodide symporter (NIS). Nucl Med Biol 29:13–18
49. Dadachova E, Nguyen A, Lin EY, Gnatovskiy L, Lu P, Pollard JW (2005) Treatment with rhenium-188-perrhenate and iodine-131 of NIS-expressing mammary cancer in a mouse model remarkably inhibited tumor growth. Nucl Med Biol 32:695–700
50. Carlin S, Akabani G, Zalutsky MR (2003) In vitro cytotoxicity of 211At-Astatide and 131I-Iodide to glioma tumor cells expressing the sodium/iodide symporter. J Nucl Med 44:1827–1838
51. Petrich T, Helmeke H-J, Meyer GJ, Knapp WH, Pötter E (2002) Establishment of radioactive astatine and iodine uptake in cancer cell lines expressing the human sodium/iodide symporter. Eur J Nucl Med Mol Imaging 29:842–854
52. Petrich T, Quintanilla-Martinez L, Korkmaz Z, Samson E, Helmeke HJ, Meyer GJ, Knapp WH, Pötter E (2006) Effective cancer therapy with the a-particle emitter [211-At]astatine in a mouse model of genetically modified sodium/iodide symporter-expressing tumors. Clin Cancer Res 12:1342–1348
53. Carlin S, Mairs RJ, Welsh P, Zalutsky MR (2002) Sodium-iodide symporter (NIS)-mediated accumulation of (211At)astatide in NIS-transfected human cancer cells. Nucl Med Biol 29:729–739